

Fig. 4. Effect of miR inhibitors on ATC cell growth. (a,b) Time course curves. The indicated cells were transfected with indicated miR inhibitors (40 pmol/well) as described in 'Materials and Methods'. The number of cells was counted at indicated times after initial transfection. * $P < 0.0001$ versus reagent only, LNA-18a and LNA-21. ** $P < 0.0001$ versus reagent only and LNA-21. (c) Dose-dependent curve. ARO cells were transfected with indicated dose of miR inhibitors (0–40 pmol/well) as described in 'Materials and Methods'. The number of cells was counted at 72 h after transfection (24 h after second transfection). * $P < 0.01$ versus LNA-18a, LNA-19a, and LNA-21. ** $P < 0.0001$ versus LNA-21a. *** $P < 0.0001$ versus LNA-18a and LNA-21. (a–c) Each point indicates the mean and SD of three wells. Similar results were obtained in three independent experiments.

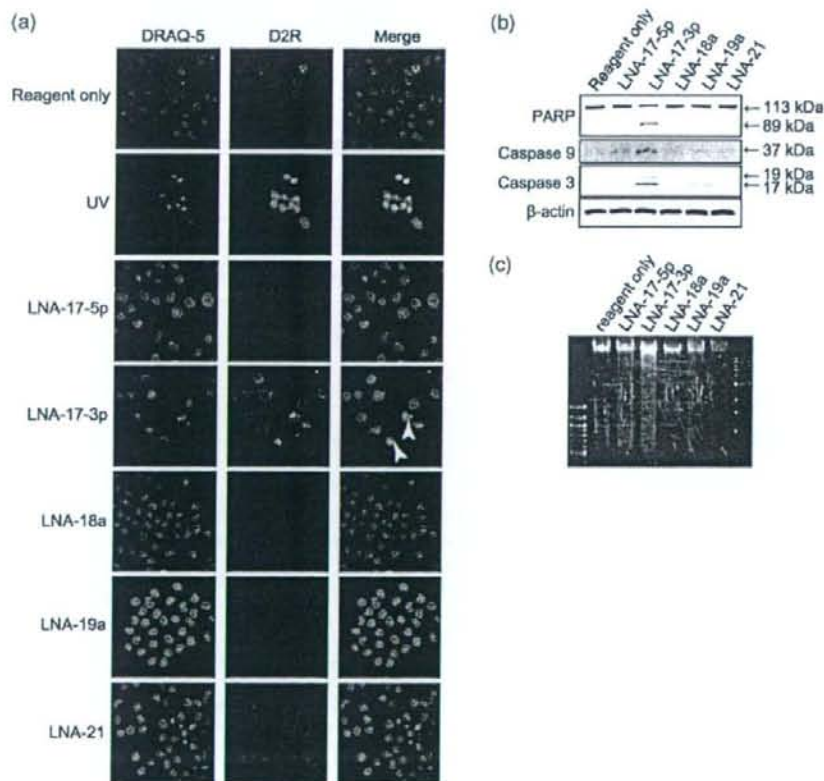


Fig. 5. Effect of miR inhibitors on apoptosis in ARO cells. ARO cells were transfected with indicated miR inhibitors. (a) Images were obtained at 72 h after transfection (24 h after second transfection). D2R and DRAQ-5 were excited with 488 and 633 nm lasers, respectively. Representative images are shown. Nuclear fragmentation is indicated by arrowhead. UV exposure was used as a positive control. (b) Cells were harvested at 72 h after transfection (24 h after second transfection), and Western blot analysis was performed using indicated primary antibodies. β -actin was used as a loading control. (c) Agarose gel electrophoresis of DNA extracted from the cells used in (b). Similar results were observed in three independent experiments.

Fig. 6. Effects of miR inhibitors on cellular senescence in ARO cells. (a) After senescence-associated β -galactosidase (SA- β -gal) staining, the number of senescent cells was counted at 72 h after transfection (24 h after second transfection). Each bar indicates the mean and SD of 10 fields. Similar results were obtained in at least two independent experiments. * $P < 0.0001$ versus others. (b) Representative images are shown. Enlarged and positively stained senescent cells are indicated by arrowheads. All images were obtained using a same magnification.

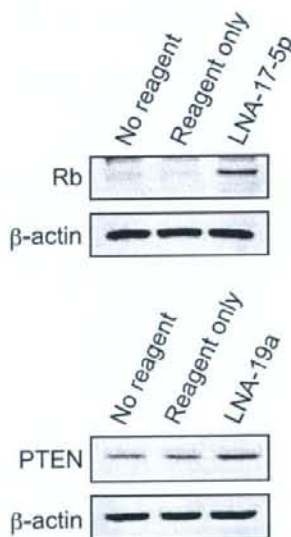
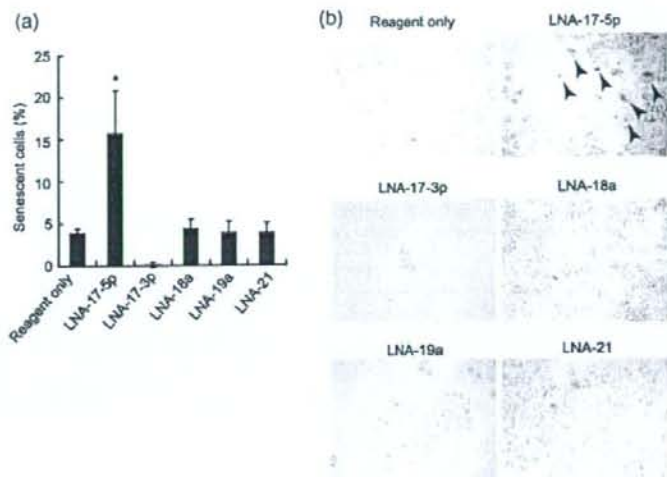


Fig. 7. Effects of miR inhibitors on target protein expression. ARO cells were transfected with indicated miR inhibitors (400 pmol in 6-cm culture dish). Cells were harvested 96 h after transfection, and Western blot analysis was performed using indicated primary antibodies. β -actin was used as a loading control. Similar results were obtained at least two independent experiments.

differences. Our results suggest that at least in some of ATC cases, the miR-17-92 cluster play a role. However, the mechanism of regulating the cluster in each case remains to be explored.

Inhibition of miR-17-3p caused apoptosis with caspase activation. Interestingly, the massive caspase activation was not observed in cells transfected with any other miR inhibitors. MiR-17-3p clearly has a distinct function from other members

of the cluster. To our knowledge, however, there is no report regarding the target mRNA of miR-17-3p. Further studies are required to clarify the function of miR-17-3p in ATC.

Although LNA-17-5p and LNA-19a induced relatively strong growth reduction, only LNA-17-5p caused some degree of cellular senescence in ARO cells. Lazzerini Denchi *et al.* have proposed that the model in which sustained E2F activity induces cellular senescence, whereas temporal E2F activation evokes cell proliferation.⁽²⁹⁾ Because MYC is overexpressed in ARO cells compared to PT,⁽³⁰⁾ inhibition of miR-17-5p and miR-20a by LNA-17-5p might cause prolonged E2F1 activation which results in cellular senescence. However, further investigation is required to clarify the detailed mechanism.

One of predicted targets for miR-19a and miR-19b is tumor suppressor PTEN.⁽³¹⁾ As expected, definite up-regulation of PTEN was observed in ARO cells transfected with LNA-19a, suggesting that one of targets of miR-19a and miR-19b is PTEN. Germline mutations of PTEN are found in patients with Cowden syndrome, which predisposes to breast and thyroid neoplasia. Recent evidence suggests that reduced expression of PTEN plays a crucial role in thyroid cancer.⁽³²⁻³⁵⁾ Moreover, Frisk *et al.* have reported that PTEN inactivation is involved in highly malignant or late-stage thyroid cancer, especially the anaplastic subtype.⁽³⁶⁾ Our results suggest that overexpression of miR-19a and miR-19b might be associated with translational suppression of PTEN and induce cell growth in ATC.

We also found overexpression of miR-106a and miR-106b, and LNA-17-5p inhibited the expression of these homologous miRNAs. Since one of the predicted targets of these miRNAs is also E2F1,⁽³¹⁾ their suppression might result in cellular senescence by the above-mentioned mechanism. Moreover, we demonstrated that the tumor suppressor RB1 was markedly up-regulated by LNA-17-5p. This is consistent with the report suggesting a post-transcriptional regulation of RB1 by miR-106a overexpression in colon cancer.⁽³⁷⁾ Therefore, up-regulation of RB1 by LNA-17-5p might result in a negative action in ATC proliferation.

When one or two of five miRNAs (miR-17-3p, miR-17-5p, miR-19a, miR-19b, and miR-20a) were inhibited, the cell growth was significantly reduced in ATC cells. On the other hand, suppression of miR-18a only moderately reduced cell growth. There is a possibility that this slight growth reduction was due to the weak binding of LNA-18a to miR-17-5p or miR-20a. Although

the expression of miR-17-5p and miR-20a was not changed after transfection with LNA-18a in the Northern blot analysis performed under denaturing conditions, LNA-18a may weakly bind to miR-17-5p or miR-20a physiologically and inhibit their function in actual live cells.

Hayashita *et al.* have reported that the miR-17-92 cluster was overexpressed in the most aggressive form of lung cancer, small-cell cancer and might play a role in its development.⁽¹⁰⁾ Very recently, Matsubara *et al.* have also demonstrated that inhibition of miR-17-5p and miR-20a caused apoptosis in lung cancer cells, whereas miR-18a and miR-19a did not show significant change in cell growth.⁽¹³⁾ The function of each miRNA in the cluster seems to be dependent on type of cells. In ATC cells, down-regulation of PTEN might be more important for cell growth as mentioned above.

In PTC, two groups have concordantly reported that miR-221 and miR-222 are overexpressed and modulate KIT expression.^(12,13) However, in our microarray data, the expression of those miRNAs in ARO cells was underexpressed. ARO cells harbor the

BRAF^{V600E} mutation and are accordingly thought to originate from PTC,⁽¹⁹⁾ suggesting that those miRNAs may play a role in PTC carcinogenesis, but are no longer critical after anaplastic transformation.

In conclusion, our results demonstrate that the miR-17-92 cluster plays an important role in cell growth in some ATC, and that miR inhibitors containing LNA efficiently block cell proliferation and even induce cell death. The miR inhibitors against miR-17-92 cluster could be a novel therapeutic approach to certain types of ATC.

Acknowledgments

This work was supported in part by a Grant-in-Aid for Scientific Research (No. 18790637 and No. 18591030) and the Global COE Program from the Ministry of Education, Culture, Sports, Science, and Technology of Japan, the President's discretionary fund of Nagasaki University, and the Nagasaki Igakudousokai Fund for medical research.

References

- Bartel DP. MicroRNAs: genomics, biogenesis, mechanism, and function. *Cell* 2004; 116: 281–97.
- Ambros V. MicroRNA pathways in flies and worms: growth, death, fat, stress, and timing. *Cell* 2003; 113: 673–6.
- Esquele-Kerscher A, Slack FJ. Oncomir – microRNAs with a role in cancer. *Nat Rev Cancer* 2006; 6: 259–69.
- Calin GA, Croce CM. MicroRNA-cancer connection: the beginning of a new tale. *Cancer Res* 2006; 66: 7390–4.
- Cimmino A, Calin GA, Fabbri M *et al.* miR-15 and miR-16 induce apoptosis by targeting BCL2. *Proc Natl Acad Sci USA* 2005; 102: 13944–9.
- Takamizawa J, Konishi H, Yanagisawa K *et al.* Reduced expression of the let-7 microRNAs in human lung cancers in association with shortened postoperative survival. *Cancer Res* 2004; 64: 3753–6.
- Johnson SM, Grosshans H, Shingara J *et al.* RAS is regulated by the let-7 microRNA family. *Cell* 2005; 120: 635–47.
- Chan JA, Krichevsky AM, Kosik KS. MicroRNA-21 is an antiapoptotic factor in human glioblastoma cells. *Cancer Res* 2005; 65: 6029–33.
- He L, Thomson JM, Hemann MT *et al.* A microRNA polycistron as a potential human oncogene. *Nature* 2005; 435: 828–33.
- Hayashita Y, Osada H, Tatematsu Y *et al.* A polycistronic microRNA cluster, miR-17-92, is overexpressed in human lung cancers and enhances cell proliferation. *Cancer Res* 2005; 65: 9628–32.
- O'Donnell KA, Wentzel EA, Zeller KI, Dang CV, Mendell JT. c-Myc-regulated microRNAs modulate E2F1 expression. *Nature* 2005; 435: 839–43.
- He H, Jazdzewski K, Li W *et al.* The role of microRNA genes in papillary thyroid carcinoma. *Proc Natl Acad Sci USA* 2005; 102: 19 075–80.
- Pallante P, Visone R, Ferracin M *et al.* MicroRNA deregulation in human thyroid papillary carcinomas. *Endocr Relat Cancer* 2006; 13: 497–508.
- Weber F, Teresi RE, Broelsch CE, Frilling A, Eng C. A limited set of human MicroRNA is deregulated in follicular thyroid carcinoma. *J Clin Endocrinol Metab* 2006; 91: 3584–91.
- Visone R, Pallante P, Vecchione A *et al.* Specific microRNAs are downregulated in human thyroid anaplastic carcinomas. *Oncogene* 2007; 26: 7590–5.
- Ain KB. Anaplastic thyroid carcinoma: behavior, biology, and therapeutic approaches. *Thyroid* 1998; 8: 715–26.
- Vini L, Harmer C. Management of thyroid cancer. *Lancet Oncol* 2002; 3: 407–14.
- Fagin JA, Matsuo K, Karmakar A, Chen DL, Tang SH, Koeffler HP. High prevalence of mutations of the p53 gene in poorly differentiated human thyroid carcinomas. *J Clin Invest* 1993; 91: 179–84.
- Kurebayashi J, Otsuki T, Tanaka K, Yamamoto Y, Moriya T, Sonoo H. Medroxyprogesterone acetate decreases secretion of interleukin-6 and parathyroid hormone-related protein in a new anaplastic thyroid cancer cell line, KTC-2. *Thyroid* 2003; 13: 249–58.
- Tanaka J, Ogura T, Sato H, Hatano M. Establishment and biological characterization of an in vitro human cytomegalovirus latency model. *Virology* 1987; 161: 62–72.
- Estour B, Van Herle AJ, Juillard GJ *et al.* Characterization of a human follicular thyroid carcinoma cell line (UCLA RO 82 W-1). *Virchows Arch B Cell Pathol Incl Mol Pathol* 1989; 57: 167–74.

- Kawabe Y, Eguchi K, Shimomura C *et al.* Interleukin-1 production and action in thyroid tissue. *J Clin Endocrinol Metab* 1989; 68: 1174–83.
- Muller PY, Janovjak H, Miserez AR, Dobbie Z. Processing of gene expression data generated by quantitative real-time RT-PCR. *Biotechniques* 2002; 32: 1372–4,6,8–9.
- Dimri GP, Lee X, Basile G *et al.* A biomarker that identifies senescent human cells in culture and in aging skin in vivo. *Proc Natl Acad Sci USA* 1995; 92: 9363–7.
- Bulgín D, Podčeko A, Takakura S *et al.* Selective pharmacologic inhibition of c-Jun NH2-terminal kinase radiosensitizes thyroid anaplastic cancer cell lines via induction of terminal growth arrest. *Thyroid* 2006; 16: 217–24.
- Chen C, Ridzon DA, Broomer AJ *et al.* Real-time quantification of microRNAs by stem-loop RT-PCR. *Nucleic Acids Res* 2005; 33: e179.
- Griffiths-Jones S, Grocock RJ, van Dongen S, Bateman A, Enright AJ. miRBase: microRNA sequences, targets and gene nomenclature. *Nucleic Acids Res* 2006; 34: D140–4.
- Trimarchi JM, Lees JA. Sibling rivalry in the E2F family. *Nat Rev Mol Cell Biol* 2002; 3: 11–20.
- Lazzarini Denchi E, Attwood C, Pasini D, Helin K. Deregulated E2F activity induces hyperplasia and senescence-like features in the mouse pituitary gland. *Mol Cell Biol* 2005; 25: 2660–72.
- Ishigaki K, Namba H, Nakashima M *et al.* Aberrant localization of beta-catenin correlates with overexpression of its target gene in human papillary thyroid cancer. *J Clin Endocrinol Metab* 2002; 87: 3433–40.
- Lewis BP, Shih IH, Jones-Rhoades MW, Bartel DP, Burge CB. Prediction of mammalian microRNA targets. *Cell* 2003; 115: 787–98.
- Weng LP, Brown JL, Eng C. PTEN coordinates G (1) arrest by down-regulating cyclin D1 via its protein phosphatase activity and up-regulating p27 via its lipid phosphatase activity in a breast cancer model. *Hum Mol Genet* 2001; 10: 599–604.
- Halachmi N, Halachmi S, Evron E *et al.* Somatic mutations of the PTEN tumor suppressor gene in sporadic follicular thyroid tumors. *Genes Chromosomes Cancer* 1998; 23: 239–43.
- Gimm O, Perren A, Weng LP *et al.* Differential nuclear and cytoplasmic expression of PTEN in normal thyroid tissue, and benign and malignant epithelial thyroid tumors. *Am J Pathol* 2000; 156: 1693–700.
- Bruni P, Boccia A, Baldassarre G *et al.* PTEN expression is reduced in a subset of sporadic thyroid carcinomas: evidence that PTEN-growth suppressing activity in thyroid cancer cells mediated by p27kip1. *Oncogene* 2000; 19: 3146–55.
- Frisk T, Foukakis T, Dwight T *et al.* Silencing of the PTEN tumor suppressor gene in anaplastic thyroid cancer. *Genes Chromosomes Cancer* 2002; 35: 74–80.
- Volinia S, Calin GA, Liu CG *et al.* A microRNA expression signature of human solid tumors defines cancer gene targets. *Proc Natl Acad Sci USA* 2006; 103: 2257–61.
- Matsubara H, Takeuchi T, Nishikawa E *et al.* Apoptosis induction by antisense oligonucleotides against miR-17-5p and miR-20a in lung cancers overexpressing miR-17-92. *Oncogene* 2007; 26: 6099–105.
- Namba H, Nakashima M, Hayaishi T *et al.* Clinical implication of hot spot BRAF mutation, V599E, in papillary thyroid cancers. *J Clin Endocrinol Metab* 2003; 88: 4393–7.

Alteration of p53-binding protein 1 expression during skin carcinogenesis: Association with genomic instability

Yuki Naruke,² Masahiro Nakashima,^{1,5} Keiji Suzuki,³ Mutsumi Matsuo-Matsuyama,² Kazuko Shichijo,² Hisayoshi Kondo⁴ and Ichiro Sekine^{1,2}

¹Tissue and Histopathology Section, Division of Scientific Data Registry, ²Department of Tumor and Diagnostic Pathology, ³Department of Molecular Medicine, ⁴Bioinformatics Section, Division of Scientific Data Registry, Atomic Bomb Disease Institute, Nagasaki University Graduate School of Biomedical Sciences, 1-12-4 Sakamoto, Nagasaki, 852-8523, Japan

(Received December 13, 2007/Revised January 21, 2008/Accepted January 23, 2008/Online publication March 13, 2008)

Epidermal cells are the first cells to be exposed to environmental genotoxic agents such as ultraviolet and ionizing radiations, which induce DNA double strand breaks (DSB) and activate DNA damage response (DDR) to maintain genomic integrity. Defective DDR can result in genomic instability (GIN) which is considered to be a central aspect of any carcinogenic process. P53-binding protein 1 (53BP1) belongs to a family of evolutionarily conserved DDR proteins. Because 53BP1 molecules localize at the sites of DSB and rapidly form nuclear foci, the presence of 53BP1 nuclear foci can be considered as a cytological marker for endogenous DSB reflecting GIN. The levels of GIN were analyzed by immunofluorescence studies of 53BP1 in 56 skin tumors that included 20 seborrheic keratosis, eight actinic keratosis, nine Bowen's disease, nine squamous cell carcinoma, and 10 basal cell carcinoma. This study demonstrated a number of nuclear 53BP1 foci in human skin tumorigenesis, suggesting a constitutive activation of DDR in skin cancer cells. Because actinic keratosis showed a high DDR type of 53BP1 immunoreactivity, GIN seems to be induced at the precancerous stage. Furthermore, invasive cancers exhibited a high level of intense, abnormal 53BP1 nuclear staining with nuclear accumulation of p53, suggesting a disruption of DDR leading to a high level of GIN in cancer cells. The results of this study suggest that GIN has a crucial role in the progression of skin carcinogenesis. The detection of 53BP1 expression by immunofluorescence can be a useful histological marker to estimate the malignant potential of human skin tumors. (*Cancer Sci* 2008; 99: 946-951)

The skin is the primary barrier for humans against the external environment. Therefore, epidermal cells are the first cells to be exposed to physical and chemical genotoxic agents such as UV and IR. IR effectively induces DSB in normal cells and activates DDR pathways to maintain genomic integrity. DDR genes, such as p53, are frequently mutated in human cancer. Thus, defective DDR can result in GIN which is generally considered to be a central aspect of any carcinogenic process.^(1,2) It has been shown that gamma irradiation induced skin tumors in mice. Most of the tumor-bearing mice showed a loss of the wild-type p53 allele. Since no skin tumor was found in wild-type p53 mice, this suggested a requirement of p53 loss in irradiation-induced skin carcinogenesis.⁽³⁾ The incidence of skin cancer was reported to be elevated in atomic bomb survivors, which also suggested a radiation etiology in human skin carcinogenesis.⁽⁴⁾

53BP1 belongs to a family of evolutionarily conserved DDR proteins with C-terminal BRCT (BRCA1 C-terminus) domains.^(5,6) The 53BP1 is a nuclear protein that rapidly localizes at the sites of DSB, and co-operatively activates p53 with other kinases.⁽⁷⁻¹²⁾ Subsequently, activated p53 plays a critical role in cellular responses to genomic injury, such as cell cycle arrest, DNA repair, and apoptosis.^(13,14) It has been well documented *in vitro* with immunofluorescence that 53BP1 exhibits diffuse nuclear staining

in untreated primary cells. However, after exposure to IR, 53BP1 localizes at the sites of DSB and forms discrete nuclear foci.^(7,8,15,16) We have recently demonstrated that immunofluorescence analysis for 53BP1 specifically detected the 53BP1 nuclear foci at the sites of DSB induced by IR in formalin-fixed paraffin-embedded mouse intestine.⁽¹⁷⁾ Because one manifestation of GIN is the induction of endogenous DSB,⁽¹⁸⁾ the level of 53BP1-focus formation can be considered as a cytological marker for GIN.

Human cancers develop through a multistep process that involves the accumulation of genetic mutations.⁽¹⁹⁾ It is well established that any DNA damages can lead to GIN and subsequently induce DDR. Thus, measurement of GIN, a hallmark feature of solid tumors that is implicated in both initiation and progression of cancers, may serve as a valuable molecular marker of malignant potential. Our recent study of thyroid tumors from patients demonstrated a few nuclear 53BP1 foci in follicular adenoma but conspicuously more nuclear 53BP1 foci in thyroid cancers. This suggested a constitutive activation of DDR in thyroid tumors and increased GIN with progression of cancer.⁽¹⁷⁾ Furthermore, anaplastic thyroid cancers prominently exhibited an abnormal and intense nuclear staining of 53BP1, which was also observed in mouse colonic crypts as a delayed response to a lethally high dose of IR, suggesting increased GIN with progression to high-grade cancer.⁽¹⁷⁾ Thus, we propose that immunofluorescence analysis of 53BP1 expression can be a useful tool to estimate the level of GIN and, simultaneously, the malignant potential of human thyroid tumors. The present study analyzed the presence of GIN by immunofluorescence of 53BP1 expression in a series of skin tissues from patients to evaluate the significance of GIN during skin carcinogenesis. Similar to thyroid tumorigenesis, GIN was shown to be induced in skin cells at a precancerous stage and increased significantly with progression to cancer.

Materials and Methods

Skin tumor tissues. A total of 56 archival skin tissue samples, which were obtained from surgically excised specimens, were selected for this study from the archives of our department (Table 1). Histologically, the 56 primary skin tumors comprised

⁵To whom all correspondence should be addressed. E-mail: moemoe@nagasaki-u.ac.jp
Abbreviations: UV, ultraviolet; IR, ionizing radiations; DSB, DNA double strand breaks; DDR, DNA damage response; GIN, genomic instability; 53BP1, P53-binding protein 1; SK, seborrheic keratosis; AK, actinic keratosis; BD, Bowen's disease; SCC, squamous cell carcinoma; BCC, basal cell carcinoma; DAPI-I, 4', 6-diamidino-2-phenylindole dihydrochloride; CIS, carcinoma *in situ*.

Brief statements: Defective DNA damage response (DDR) can result in genomic instability (GIN) which is considered to be a central aspect of any carcinogenic process. P53-binding protein 1 (53BP1) belongs to a family of evolutionarily conserved DDR proteins. This study demonstrated a number of nuclear 53BP1 foci in human skin tumorigenesis, suggesting a constitutive activation of DDR in skin cancer cells. The results of this study suggest that GIN has a crucial role in the progression of skin carcinogenesis.

Table 1. Summary of subjects used in this study

Histological type	n	Mean age (range)	M/F	Site (nonexposed/sun-exposed)
Normal epidermis				
non-exposed	14	60.8 (31–80)	11/3	14/0
sun-exposed	8	79.9 (66–88)	3/5	0/8
Seborrheic keratosis				
non-exposed	10	65.6 (58–90)	10/0	10/0
sun-exposed	10	77.9 (53–91)	3/7	0/10
Actinic keratosis	8	79.5 (66–91)	3/5	0/8
Bowen's disease	9	76.5 (66–88)	3/6	1/8
Squamous cell carcinoma	9	82.3 (74–96)	3/6	0/8
Basal cell carcinoma	10	73.3 (53–89)	5/5	3/7

the following: 20 SK arising from 10 sun-exposed (including seven faces and three necks) and 10 non-exposed sites (including four abdomens, three chests, two axillae, and one back); eight AK; nine BD; nine SCC; and 10 BCC. All samples were formalin-fixed paraffin-embedded tissues, from which sections were prepared for immunofluorescence studies. For normal controls, 14 samples of non-exposed (including five abdomens, five backs, two ramps, one chest, and one axilla) and eight samples of sun-exposed (including five faces, one neck, one hand, and one leg) normal epidermal cells surrounding tumor sections were evaluated.

Immunofluorescence. After antigen retrieval with microwave treatment in citrate buffer, deparaffinized sections were preincubated with 10% normal goat serum. Tissue sections were then reacted with anti-53BP1 rabbit polyclonal antibody (Bethyl Laboratories, Montgomery, TX, USA) at a 1:200 dilution. The slides were subsequently incubated with Alexa Fluor 488-conjugated goat anti-rabbit antibody (Invitrogen, Carlsbad, CA, USA). Specimens were counterstained with DAPI-I (Vysis, Downers Grove, IL, USA), and were visualized and photographed using a fluorescence microscope (Zeiss Axioplan2; Carl Zeiss Japan, Tokyo, Japan) equipped with a charge coupled device (CCD) camera, and then analyzed with IPLab/MAC image software (Scanalytics, Fairfax, VA, USA). Signals were analyzed in 10 viewing areas per case at a 1000-fold magnification.

Evaluation of immunofluorescence results. As described in our previous report,⁽¹⁷⁾ the pattern of 53BP1 immunoreactivity was classified into four types: (1) stable type: faint and diffuse nuclear staining; (2) low DDR type: one or two discrete nuclear foci; (3) high DDR type: three or more discrete nuclear foci; and (4) abnormal type: intense heterogeneous nuclear staining, occasionally, with several small foci. The percentage of epidermal or tumor cells expressing each type of 53BP1 immunoreactivity in each viewing area was graded into the following four groups: (1) negative: 0 to less than 5%; (2) low: 5% to less than 30%; (3) medium: 30% to 60%; and (4) high:

more than 60%. The type of 53BP1 expression pattern in each case was determined by the predominant expression pattern.

Statistical analysis. The Mann-Whitney test was used to assess differences in the type of 53BP1 expression between non-exposed and exposed epidermal cells. Spearman's correlation coefficient by rank test was used to assess correlation between histological type of skin tumors and type of 53BP1 expression. A *P*-value of less than 0.05 was considered statistically significant.

Double-labeled immunofluorescence. To assess the colocalization of 53BP1-foci formation and p53 expression, double-labeled immunofluorescence was performed. We also carried out a double-labeled immunofluorescence of 53BP1 and Ki-67 expression to clarify the association of type of 53BP1 expression and cycling tumor cells. In double staining, tissues were incubated with a mixture of rabbit anti-53BP1 antibody and mouse anti-p53 monoclonal antibody (DO7; Dako, Glostrup, Denmark) at a 1:200 dilution or mouse anti-Ki-67 monoclonal antibody (MIB-1; Dako) at a 1:50 dilution, and subsequently incubated with a mixture of Alexa Fluor 488-conjugated goat anti-rabbit antibody and Alexa Fluor 546-conjugated goat anti-mouse antibody. Specimens were counterstained with DAPI-I (Vysis), and were visualized and photographed using a fluorescence microscope (Zeiss Axioplan2) equipped with a CCD camera, and then analyzed with IPLab/MAC image software (Scanalytics). Signals were analyzed at a 1000-fold magnification.

Results

53BP1 expression in normal epidermis surrounding tumors. Of the 14 controls consisting of nonexposed normal epidermis, 13 cases (92.9%) expressed only stable type cells (Fig. 1a), while one case (7.1%) showed stable type keratinocytes but also included a small number (up to 10%) of low DDR type in the basal layer. Of the other eight controls consisting of sun-exposed normal epidermis, two cases (20%) expressed only stable type cells, while five cases (62.5%) showed stable type in more than 70% of keratinocytes but also had up to 30% of low DDR type (Fig. 1b) in the basal layer. One other case (12.5%) also showed stable type in more than 70% of keratinocytes, but included up to 30% of high DDR type in the basal layer.

53BP1 expression in skin tumors. The results of the immunofluorescence of staining patterns for 53BP1 in each histological type of skin tumors are presented in Table 2. Similar to the pattern observed for normal epidermal cells, all 10 of the non-exposed SK cases expressed only the stable type (Fig. 2a). Of the 10 sun-exposed SK cases, four (40%) expressed only the stable type, while six (60%) showed stable type in more than 70% of tumor cells, but also up to 30% of low DDR type (Fig. 2b) mainly in the basal layer.

In contrast to the normal epidermis and SK, of the eight AK cases, four cases (50%) and three cases (37.5%) showed high DDR (Fig. 2c) and low DDR types, respectively, in dysplastic cells, while only one case (12.5%) expressed the stable type.

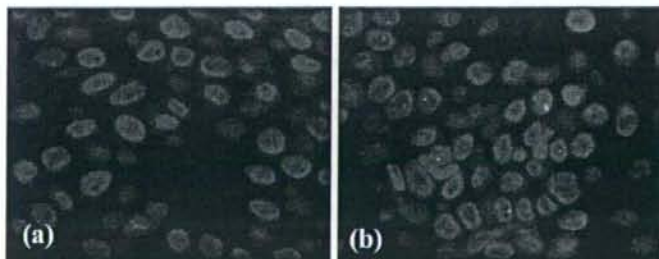


Fig. 1. Immunofluorescence of p53-binding protein 1 (53BP1) expression in the normal epidermis surrounding tumor sections. (a) The non-exposed epidermis showed a stable type staining and rarely one nuclear focus. (b) Sun-exposed epidermis occasionally showed one discrete 53BP1 nuclear focus at the basal layer.

Table 2. Results for type of p53-binding protein 1 (53BP1) expression in skin tumors by immunofluorescence

	n	Stable	Low DDR	High DDR	Mixed DDR and abnormal	Abnormal
Epidermis						
non-exposed	14	13 (92.9%)	1 (7.1%)	0	0	0
sun-exposed	8	2 (25.0%)	5 (62.5%)	1 (12.5%)	0	0
SK						
non-exposed	10	10	0	0	0	0
sun-exposed	10	4 (40.0%)	6 (60.0%)	0	0	0
AK	8	1 (12.5%)	3 (37.5%)	4 (50.0%)	0	0
BD	9	1 (11.1%)	2 (22.2%)	4 (44.4%)	2 (22.2%)	0
SCC	9	0	0	0	4 (44.4%)	5 (55.6%)
BCC	10	0	0	0	1 (10.0%)	9 (90.0%)

DDR, DNA damage response; SK, seborrheic keratosis; AK, actinic keratosis; BD, Bowen's disease; SCC, squamous cell carcinoma; BCC, basal cell carcinoma.

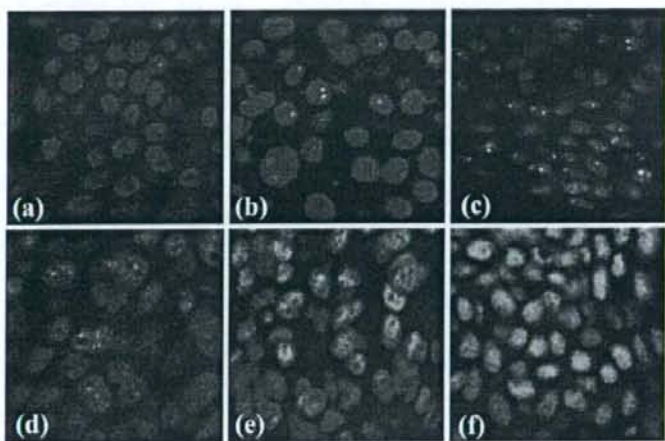


Fig. 2. Immunofluorescence of p53-binding protein 1 (53BP1) expression in human skin tumors. (a) Seborrheic keratosis (SK) in the non-exposed skin expressed stable type staining with rarely one nuclear focus (stable type), (b) whereas SK in the sun-exposed skin expressed an occasional one or two nuclear foci (low DNA damage response (DDR) type). (c) Actinic keratosis showed three or more discrete nuclear foci in dysplastic cells (high DDR type). (d) Bowen's disease showed several discrete nuclear foci mixed with intense and heterogeneous nuclear staining (mixed DDR and abnormal type). (e) Squamous cell carcinoma as well as (f) basal cell carcinoma exhibited intense and heterogeneous nuclear staining (abnormal type).

In the nine BD cases, two cases (22.2%) showed low DDR type, four cases (44.4%) were of high DDR type, and two cases (22.2%) were of mixed high DDR and abnormal type (Fig. 2d), while only one case (11.1%) expressed the stable type. Of the nine SCC cases, four (44.4%) were of mixed low DDR and abnormal type and five (55.6%) were of the abnormal type (Fig. 2e). Finally, of the 10 BCC cases, one case (10%) was of mixed low DDR and abnormal type, and nine cases (90%) were of the abnormal type (Fig. 2f).

The Mann-Whitney test revealed that DDR expression of 53BP1 was significantly higher in the sun-exposed epidermis than in the non-exposed epidermis ($P = 0.001$). Furthermore, Spearman's analysis revealed that the histological type of skin tumors was significantly correlated with type of 53BP1 expression ($P < 0.001$).

Double-labeled immunofluorescence of 53BP1 and p53 expressions (Fig. 3)/Ki-67 expressions (Fig. 4). The normal epidermis and SK expressed the stable or a low DDR type of 53BP1 immunoreactivity and only a few Ki-67 nuclear stainings at the basal layer but no p53 nuclear staining. Discrete nuclear foci in a high DDR type of 53BP1 immunoreactivity were observed and were colocalized to dysplastic cells exhibiting p53 nuclear staining at the basal layer in AK. In BD, p53 nuclear staining was sparsely found in cancer cells which were distributed throughout the epidermal layer, and discrete nuclear foci of high DDR type of 53BP1 immunostaining were colocalized to p53-positive cancer

cells. In SCC and BCC, high levels of abnormal type of 53BP1 and strong p53 immunoreactivity were observed in nuclei of cancer cells, and cells expressing the abnormal type of 53BP1 immunoreactivity were randomly distributed in lesions. Intense 53BP1 staining was not always colocalized with p53 overexpression in cancer cells. Furthermore, double staining of 53BP1 and Ki-67 demonstrated that discrete nuclear foci of 53BP1 immunostaining were not colocalized to Ki-67-positive dysplastic/cancer cells in AK/BD; whereas abnormal type of 53BP1 staining frequently expressed Ki-67 nuclear staining.

Discussion

Development of SCC of the skin is viewed as a multistep process, while BCCs are believed to develop *de novo*.⁽²⁰⁾ In skin carcinogenesis, AK is a well established precancerous skin lesion and it has been suggested that ~10% of these sun-induced lesions will develop into SCC.⁽²¹⁾ BD, also known as CIS, represents a preinvasive stage of SCC. The present study demonstrated apparent differences in 53BP1 staining patterns during human skin tumorigenesis, as in the following: SK/benign tumor, AK/precancerous lesion, BD/CIS, and SCC or BCC/invasive cancer. The number of discrete immunoreactive nuclear foci in DDR type of 53BP1 in the epidermis seems to increase in precancerous lesions. Furthermore, the abnormal type of 53BP1 immunoreactivity was restricted to malignancies

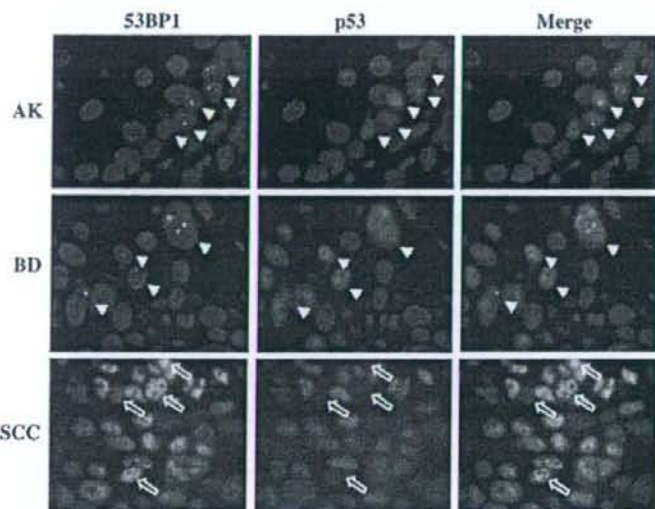


Fig. 3. Double-labeled immunofluorescence for p53-binding protein 1 (53BP1) and p53 expression. Actinic keratosis (AK) showed colocalization of discrete 53BP1 nuclear foci and p53 nuclear staining in dysplastic cells at the basal layer, suggesting an activation of DNA damage response (DDR). Bowen's disease (BD) also showed colocalization of discrete 53BP1 nuclear foci and p53 nuclear staining in dysplastic cells including dispersed plump cells. Squamous cell carcinoma (SCC) exhibited intense and heterogeneous nuclear staining of both 53BP1 and p53 immunoreactivity; however, intense 53BP1 staining was not always colocalized with p53 overexpression, suggesting a disruption of the DDR pathway. Arrows indicate colocalization of 53BP1 nuclear foci and p53 staining in both AK and BD. Open arrows indicate cancer cells showing intense 53BP1 staining with no p53 staining in SCC.

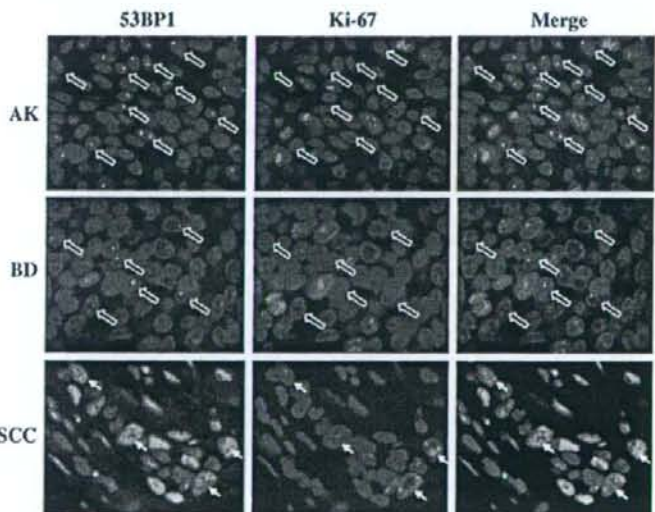


Fig. 4. Double-labeled immunofluorescence for p53-binding protein 1 (53BP1) and Ki-67 expression. Actinic keratosis (AK) showed no colocalization of discrete 53BP1 nuclear foci and Ki-67 nuclear staining at the basal layer. Bowen's disease (BD) also showed independent discrete 53BP1 nuclear foci from Ki-67 nuclear staining in cancer cells. Squamous cell carcinoma (SCC) occasionally exhibited intense and heterogeneous nuclear staining of both 53BP1 and Ki-67 immunoreactivity, suggesting a proliferating ability through a disruption of the DDR pathway. Open arrows indicate cells showing 53BP1 nuclear foci with no Ki-67 staining in both AK and BD. Arrows indicate colocalization of intense 53BP1 staining and Ki-67 staining in SCC.

including both CIS and invasive cancers. Similar results, which showed the differences in 53BP1 expression patterns during carcinogenesis, were also obtained in our recent study on thyroid tumors resected from patients.⁽¹⁷⁾ Therefore, we submit that immunofluorescence analysis of 53BP1 expression can be a useful tool to estimate the level of GIN and, simultaneously, the malignant potential of human tumors such as skin and thyroid tumors.

Interestingly, the low DDR type of 53BP1 immunoreactivity was very rare in the non-exposed epidermis but frequently found in sun-exposed skin. Similarly, sun-exposed SK/benign skin tumors also frequently showed a low DDR type of 53BP1 immunoreactivity, but none of the nonexposed SK cases

expressed the DDR type of 53BP1 immunoreactivity. Because the skin is the primary barrier for humans against the external environment, sun-exposed epidermis is continuously exposed to a low level of physical and chemical genotoxic agents such as UV and IR. Thus, a low DDR type of 53BP1 immunoreactivity in the sun-exposed epidermis may represent a minor genotoxic injury induced by external environmental factors.

p53 is activated by DDR-associated molecules, and is essential to control GIN and to suppress tumorigenesis.⁽²²⁾ The p53 mutation is the most prominent aberration in skin cancers, and it is now established that ~50% of all skin cancers show p53 mutations.⁽²³⁾ Double-labeled immunofluorescence was carried out to evaluate the association between the type of 53BP1

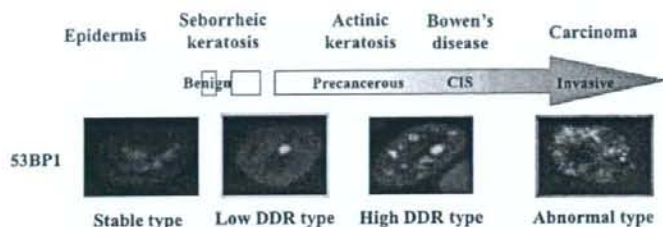


Fig. 5. Schematic presentation showing differences in p53-binding protein 1 (53BP1) staining patterns during skin tumorigenesis. DDR, DNA damage response; CIS, carcinoma *in situ*.

expression and p53 nuclear staining. In this study, although no p53 staining was observed in the epidermis and SK even at the sun-exposed sites which showed a low DDR type of 53BP1 immunoreactivity, AK showed both p53 nuclear staining and a high DDR type of 53BP1 immunoreactivity in dysplastic cells at the basal layer in the epidermis. The colocalization of p53 nuclear staining and 53BP1 nuclear foci was also observed in BD. P53 mutations have been found in precancerous epidermis,⁽²⁴⁻²⁶⁾ and can be detected by immunohistochemistry. Indeed, 70% of immunohistochemical detections were shown to have an underlying mutation in the p53 gene.^(25,27) Because of the loss of p53 function based on gene mutation, environmental genotoxic agents may easily induce DSB in precancerous lesion/CIS in skin. Alternatively, because this study also demonstrated no colocalization of DDR type 53BP1 expression and Ki-67 nuclear staining as a marker for cycling cells in AK and BD, activated DDR induced by genotoxic factors may activate p53 function to induce cell-cycle arrest in injured cells. Furthermore, a high level of the abnormal type of 53BP1 immunoreactivity was restricted to invasive cancer and was significantly associated with p53 overexpression reflecting mutation. However, cancer cells exhibiting an abnormal type of 53BP1 staining were colocalized with Ki-67 staining but not always colocalized with p53 staining. Thus, cancer cells expressing strong p53 immunoreactivity were cycling cells, suggesting a loss of p53 function and a disruption of the DDR pathway; whereas AK and BD cells exhibiting both 53BP1 nuclear foci and weak p53 staining were non-cycling cells, suggesting a p53 function through the activated DDR pathway. Taken together, these findings may indicate that

GIN may have already occurred at the precancerous stage during skin tumorigenesis, and that a loss of control of GIN based on p53 mutations may allow further accumulation of other genomic alterations to progress to invasive cancer through acceleration of cell proliferating.

In summary, this study demonstrated a number of nuclear 53BP1 foci in skin tumors resected from patients, which were similar to those found in irradiated cells, suggesting a constitutive activation of DDR in skin cancer cells. Because AK showed a high DDR type of 53BP1 immunoreactivity which colocalized with p53 nuclear staining as well as BD, GIN seems to be induced at the precancerous stage. Furthermore, invasive cancers exhibited the abnormal type of 53BP1 immunoreactivity with an underlying mutation in the p53 gene and an increased proliferation, suggesting disrupted DDR subsequently leading a high level of GIN in cancer cells. This study proposed that GIN has a crucial role in the progression of skin carcinogenesis. Immunofluorescence analysis of 53BP1 expression of various tumor tissues should be performed to clarify the significance of 53BP1 staining pattern as a common histological marker to estimate the malignant potential of human tumors.

Acknowledgments

This work was supported in part through Nagasaki University Global Center of Excellence program 'Global Strategic Center for Radiation Health Risk Control' and by a Grant-in-Aid for Scientific Research from the Ministry of Education, Culture, Sports, Science, and Technology of Japan. (No. 18590334).

References

- Lengauer C, Kinzler KW, Vogelstein B. Genetic instabilities in human cancers. *Nature* 1998; 396: 643-9.
- Coleman WB, Tsongalis GJ. The role of genomic instability in human carcinogenesis. *Anticancer Res* 1999; 19: 4645-64.
- Miyazawa T, Sato H, Hatakeyama K, Kitagawa T, Kominami R. Allelic losses in mouse skin tumors induced by gamma-irradiation of p53 heterozygotes. *Jpn J Cancer Res* 2002; 93: 994-9.
- Sadamori N, Mine M, Hori M. Skin cancer among atom bomb survivors. *Lancet* 1989; 1: 1267.
- Bork P, Hofmann K, Bucher P, Neuwald AF, Altschul SF, Koonin EV. A superfamily of conserved domains in DNA damage-responsive cell cycle checkpoint proteins. *FASEB J* 1997; 11: 68-76.
- Joo WS, Jeffrey PD, Cantor SB, Finnin MS, Livingston DM, Pavletich NP. Structure of the 53BP1 BRCT region bound to p53 and its comparison to the Brc1 BRCT structure. *Genes Dev* 2002; 16: 583-93.
- Ward JM, Minn K, Jorda KG, Chen J. Accumulation of checkpoint protein 53BP1 at DNA breaks involves its binding to phosphorylated histone H2AX. *J Biol Chem* 2003; 278: 19579-82.
- Schultz LB, Chehab NH, Malikzay A, Halazonetis TD. p53 binding protein 1 (53BP1) is an early participant in the cellular response to DNA double-strand breaks. *J Cell Biol* 2000; 151: 1381-90.
- Rappold I, Iwabuchi K, Date T, Chen J. Tumor suppressor p53 binding protein 1 (53BP1) is involved in DNA damage-signaling pathways. *J Cell Biol* 2001; 153: 613-20.
- Anderson L, Henderson C, Adachi Y. Phosphorylation and rapid relocalization of 53BP1 to nuclear foci upon DNA damage. *Mol Cell Biol* 2001; 21: 1719-29.
- Xia Z, Morales JC, Dunphy WG, Carpenter PB. Negative cell cycle regulation and DNA damage-inducible phosphorylation of the BRCT protein 53BP1. *J Biol Chem* 2001; 276: 2708-18.
- Shiloh Y, Kastan MB. ATM: genome stability, neuronal development, and cancer cross paths. *Adv Cancer Res* 2001; 83: 209-54.
- Xu Y, Baltimore D. Dual roles of ATM in the cellular response to radiation and in cell growth control. *Genes Dev* 1996; 10: 2401-10.
- Xu Y, Yang EM, Brugarolas J, Jacks T, Baltimore D. Involvement of p53 and p21 in cellular defects and tumorigenesis in *Atm*^{-/-} mice. *Mol Cell Biol* 1998; 18: 4385-90.
- Mochan TA, Venerer M, DiTullio RA Jr, Halazonetis TD. 53BP1 and NFB1/MDC1-Nbs1 function in parallel interacting pathways activating ataxia-telangiectasia mutated (ATM) in response to DNA damage. *Cancer Res* 2003; 63: 8586-91.
- Rakhorst HA, Tra WM, Posthumus-Van Sluijs ST *et al*. Quantitative analysis of radiation-induced DNA break repair in a cultured oral mucosal model. *Tissue Eng* 2006; 12: 3395-403.
- Nakashima M, Suzuki K, Meirmanov S *et al*. Foci formation of p53-binding protein 1 in thyroid tumors: activation of genomic instability during thyroid carcinogenesis. *Int J Cancer* 2008; 122: 1082-8.
- Suzuki K, Yokoyama S, Waseda S, Kodama S, Watanabe M. Delayed reactivation of p53 in the progeny of cells surviving ionizing radiation. *Cancer Res* 2003; 63: 936-41.

- 19 Hahn WC, Weinberg RA. Modelling the molecular circuitry of cancer. *Nat Rev Cancer* 2002; 2: 331–41.
- 20 Boukamp P. Non-melanoma skin cancer: what drives tumor development and progression? *Carcinogenesis* 2005; 26: 1657–67.
- 21 Johnson TM, Rowe DE, Nelson BR, Swanson NA. Squamous cell carcinoma of the skin (excluding lip and oral mucosa). *J Am Acad Dermatol* 1992; 26: 467–84.
- 22 DiTullio RA Jr, Mochan TA, Venere M *et al*. 53BP1 functions in an ATM-dependent checkpoint pathway that is constitutively activated in human cancer. *Nat Cell Biol* 2002; 4: 998–1002.
- 23 Giglia-Mari G, Sarasin A. TP53 mutations in human skin cancers. *Hum Mutat* 2003; 21: 217–28.
- 24 Nakazawa H, English D, Randell PL *et al*. UV and skin cancer: specific p53 gene mutation in normal skin as a biologically relevant exposure measurement. *Proc Natl Acad Sci USA* 1994; 91: 360–4.
- 25 Jonason AS, Kunala S, Price GJ *et al*. Frequent clones of p53-mutated keratinocytes in normal human skin. *Proc Natl Acad Sci USA* 1996; 93: 14025–9.
- 26 Ling G, Persson A, Berne B, Uhlen M, Lundeberg J, Ponten F. Persistent p53 mutations in single cells from normal human skin. *Am J Pathol* 2001; 159: 1247–53.
- 27 Ren ZP, Ponten F, Nister M, Ponten J. Two distinct p53 immunohistochemical patterns in human squamous-cell skin cancer, precursors and normal epidermis. *Int J Cancer* 1996; 69: 174–9.

Supplementary material

The following supplementary material is available for this article:

Table S1. Odds ratio (OR) and 95% confidence interval (CI) for the incidence of DNA damage response expression of 53BP1 in both normal epidermis and seborrheic keratosis samples.

This material is available as part of the online article from:

<http://www.blackwell-synergy.com/doi/abs/10.1111/j.1349-7006.2008.00786.x>

(This link will take you to the article abstract).

Please note: Blackwell Publishing are not responsible for the content or functionality of any supplementary materials supplied by the authors. Any queries (other than missing material) should be directed to the corresponding author for the article.

Short Communication

Association between C677T/MTHFR genotype and homocysteine concentration in a Kazakh population

Ainur Akilzhanova MD PhD¹, Noboru Takamura MD PhD², Yosuke Kusano MD PhD³,
Ludmila Karazhanova MD PhD¹, Shunichi Yamashita MD PhD², Hiroshi Saito MD PhD²
and Kiyoshi Aoyagi MD PhD²

¹Department of Therapy №2, Semipalatinsk State Medical Academy, Semipalatinsk, Republic of Kazakhstan
²Nagasaki University Graduate School of Biomedical Sciences, Nagasaki, Japan and ³Nagasaki Wesleyan University, Nagasaki, Japan

We recently suggested that due to insufficient intake of vegetables, low folate status and mild homocysteinemia might exist in the Kazakh population. To clarify the determinants of homocysteine concentrations among this population, we determined concentrations of serum folate, albumin, creatinine, vitamin B₁₂, and the C677T/MTHFR genotype in 110 Kazakh individuals and compared these with plasma total homocysteine. In Kazakh, after adjustment for age and sex, folate was correlated with plasma total homocysteine, whereas concentrations in those with the TT genotype was almost twice as high as in those with the CC and CT genotypes (19.7±1.8 mol/L vs. 10.7±0.5 mol/L, $p < 0.001$). Our results suggest that the C677T/MTHFR genotype is associated with homocysteine concentrations in this population and this association might be affected by other factors, such as folate status.

Key Words: folate, homocysteine, Kazakh, 5,10-methylenetetrahydrofolate reductase

INTRODUCTION

Awareness of the health benefits of folate intake has considerably increased; research has shown that insufficient levels of this vitamin may contribute to neural tube defects such as spina bifida and Down syndrome.¹ Periconceptional daily supplementation with synthetic folic acid has been recommended in many developed countries.² Results of intervention studies have shown that periconceptional use of folic acid supplements alone, or multivitamins combined with folic acid, can lower the risk of neural tube defects by 40% to 80%.³

Also, it is well known that folate influences homocysteine (Hcy) metabolism as a cosubstrate,⁴ and elevated plasma total Hcy is an independent risk factor for cardiovascular disease (CVD) and stroke.⁵ Data from several, but not all, prospective studies show a reduced risk of CVD and stroke associated with high intakes or blood concentration of folate.⁵

In addition to folate intake, plasma Hcy levels are regulated mainly by 5,10-methylenetetrahydrofolate reductase (MTHFR), which is involved in the folate-dependent remethylation of Hcy.^{6,7} In particular, the 677 C to T polymorphism of the MTHFR gene (C677T/MTHFR) has been investigated most extensively in relation to its effects on the total Hcy (tHcy) concentration. The prevalence of C677T/MTHFR is relatively high in the general population. It was reported that the prevalence of this allele is 0.34 (0.29-0.39) in whites, 0.42 (0.34-0.50) in the Japanese, and 0.08 (0.06-0.12) in Africans,⁸ but there is no report on its frequency in the Kazakh.

Recently, we showed that folate deficiency might exist among the Kazakhs, probably due to their traditional diet.^{9,10} We screened serum folate and plasma Hcy in the general population of Kazakh adults, and fifty of 61 (82.0%) people tested, showed low concentrations of folate. In order to reduce the risk of neural tube defects and future cardiovascular disease due to atherosclerosis, supplementation of folic acid is definitely needed in Kazakhstan. However, for the appropriate implementation of this health policy, identification of Hcy determinants in the Kazakh population is needed.

In this study, we screened biochemical and genetic markers linked to folate and Hcy metabolism in order to identify the determinants of Hcy concentration among the Kazakhs. The results obtained should be useful for future folic acid supplementation in a population with a low folate status.

MATERIALS AND METHODS

Prior to this study, ethical approval was obtained from the special committee of Semipalatinsk State Medical Academy. We collected blood samples in Semipalatinsk, Republic of Kazakhstan. Before the study, participants with

Corresponding Author: Dr Noboru Takamura, Department of Public Health, Nagasaki University Graduate School of Biomedical Sciences, 1-12-4 Sakamoto, Nagasaki 852-8523, Japan

Tel: +81-95-849-7066; Fax: +81-95-849-7069

Email: takamura@nagasaki-u.ac.jp

Manuscript received 13 August 2007. Initial review completed 7

September 2007. Revision accepted 17 January 2008.

an apparent past or present history of atherosclerotic diseases (including cerebral infarction or hemorrhage or ischemic heart disease), current pregnancy, psoriasis, seizures, or use of methotrexate or phenytoin were excluded. After these exclusions, 110 healthy Kazakh adults (61 men and 49 women, age 20-77 years) were included in this study. The average age was 37.9 ± 16.1 years. For comparison, we also analyzed serum folate, plasma tHcy levels, and *C677T/MTHFR* genotype with the same protocol in 110 sex- and age-matched volunteers from the Japanese general population (61 men and 49 women, age 20-76 years), who were recruited during the "National Insurance Health-Up Project" performed at Nagasaki Prefecture, Japan. Before the study, written informed consent was obtained from all participants.

Fasting blood samples were obtained, and after the separation from whole blood, serum and plasma were kept at -20°C and -80°C until assay, respectively. Serum folate and vitamin B₁₂ (VB₁₂) were measured using chemiluminescent immunoassay radioimmunoassay methods. Serum creatinine and albumin were measured by enzyme and BCG methods, respectively. Plasma tHcy was measured using high performance liquid chromatography. The normal ranges of serum folate, VB₁₂, creatinine, and albumin were 3.6-12.9 g/L, 233-914 ng/L, 6.5-10.9 mg/L, and 3.7-5.5 g/dL, respectively. The normal range of plasma tHcy was 6.3-8.9 mol/L in men and 5.1-11.7 mol/L in women.

Genomic DNA was automatically extracted from blood cells separated from plasma using a MagExtractor MFX[®] (TOYOBO, Osaka, Japan). For the determination of *C677T/MTHFR* genotypes, we used the TaqMan polymerase chain reaction (PCR) method (Applied Biosystems Japan, Tokyo, Japan). In the current investigation, we prepared 2 probes: the C allele-specific probe, 5' - Tct-TCT GCC GGA GcC GAT TTC ATC ATC - Tamra-3', and the T allele-specific probe, 5' - Fam-TCT GCG GGA Gic GAT TTC ATC ATC - Tamra-3'. The primer

design for PCR of the flanking region of *C677T/MTHFR* was as follows: forward, 5' - CTG GGA AGA ACT CAG CGA AC - 3'; reverse, 5' - GGA AGG TGC AAG ATC AGA GC - 3'. PCR was carried out with a thermal cycler (Bio-Rad Laboratories, Hercules, USA). PCR was performed according to the following conditions: initial denaturation at 95°C for 10 minutes, followed by 35 cycles of 95°C for 15 seconds and 60°C for 60 seconds. The fluorescence level of PCR products was measured with an ABI PRISM 7900 Sequence Detector (Applied Biosystems Japan, Tokyo, Japan), resulting in clear identification of the three *C677T/MTHFR* genotypes (CC, CT, and TT).

Since tHcy levels were skewedly distributed, logarithmic transformation was performed for the following statistical analysis. Multiple linear regression analysis was performed for the identification of determinants of tHcy levels, adjusted for age and sex. Average values \pm S.D. for men ($n=49$) and women ($n=61$), and multiple linear regression analysis for the association with plasma tHcy levels after adjustment for age and sex were determined. Furthermore, the tHcy level of each *C677T/MTHFR* genotype adjusted by age and sex was evaluated with the use of the ANCOVA test.

A probability value of less than 0.05 was considered to indicate significance. All statistical analyses were performed with SPSS 14.0[®] (SPSS Japan Inc., Tokyo, Japan).

RESULTS AND DISCUSSION

Serum folate concentrations of the Kazakh participants ranged from 0.7 to 13.5 g/L and 72 of 110 (65.4%), which indicated low folate concentrations (<3.6 g/L). Plasma tHcy levels of the Kazakh participants ranged from 5.5 to 41.1 mol/L. Multiple regression analysis adjusted by age and sex showed that serum creatinine and albumin did not correlate with plasma tHcy concentration. Serum VB₁₂ was relatively correlated with tHcy ($\beta=0$, $p=0.076$, Table 2) and serum folate was significantly cor-

Table 1. Clinical characteristics of the Kazakh and Japanese study participants.

	Kazakh	Japanese	p-value†
Age (yrs)	37.9±16.1	38.1±14.9	0.92
tHcy‡ (μmol/L)	11.4±6.0	11.7±3.4	0.09
Creatinine (mg/L)	7.3±1.2	7.0±1.7	0.01
Vitamine B12 (ng/L)	337.8±110.9	310.9±90.2	0.24
Folate (μg/L)	3.6±2.1	10.4±5.3	<0.001
Albumin (g/dL)	4.8±0.3	4.6±0.3	0.67

† Data are expressed as mean \pm S.D. Differences between the Kazakh and Japanese were evaluated by Mann-Whitney's U test.

‡ tHcy: total homocysteine

Table 2. Multiple linear regression analysis for the association with plasma log (tHcy) levels after adjustment for age and sex.

	Kazakh			Japanese		
	β †	95%CI†	p-value	β	95%CI	p-value
Creatinine (mg/L)	0.41	-0.14,0.96	0.14	0.26	0.18,0.35	0.01
Vitamin B12 (ng/L)	0	-0.001,0	0.076	0	-0.002,0.001	0.089
Folate (μg/L)	-0.26	-0.034,-0.006	0.007	0.01	0,0.003	0.060
Albumin (g/dL)	0.091	-0.077,0.26	0.28	0.099	-0.080,0.28	0.30

† The regression coefficient (β) is the average amount that the dependent variable increases when the independent variable increases by one unit and other variables are held constant.

‡ 95% confidence interval (CI) represents the plus/minus range around the observed sample regression coefficients. If the coefficient interval includes 0, there is no significant

Table 3. Plasma tHcy concentrations by C677T/MTHFR genotype in the Kazakh and Japanese

	MTHFR Genotype		p-value
	TT	CC&CT	
<i>Not adjusted</i>			
Kazakh			
log not transformed	19.5±1.8†	9.7±0.5	<0.001
log transformed	1.2±0.05	1.0±0.02	<0.001
Japanese			
log not transformed	12.6±0.6	11.6±0.2	0.13
log transformed	1.1±0.02	1.1±0.01	0.11
<i>Age and sex adjusted</i>			
Kazakh			
log not transformed	19.7±1.8	9.7±0.5	<0.001
log transformed	1.2±0.05	1.0±0.015	<0.001
Japanese			
log not transformed	12.7±0.6	11.6±0.2	0.09
log transformed	1.1±0.02	1.1±0.01	0.08

†Values are expressed as mean ± standard deviation

related with tHcy ($\beta = -0.26, p < 0.01$).

The frequencies of C677T/MTHFR genotypes were 41.8% for CC, 44.5% for CT, and 13.7% for TT in the Kazakh. With regard to the Japanese, the frequencies were 36.4% for CC, 48.1% for CT, and 15.5% for TT. Plasma tHcy levels in participants with the TT genotype were significantly higher than those in participants with CC and CT genotypes (19.5±1.8 mol/L vs. 9.7±0.5 mol/L; $p < 0.001$; Table 3). When adjusted by age and sex, tHcy levels in the TT genotype were almost twice as high as in subjects with CC and CT genotypes in the Kazakh (19.7±1.8 mol/L vs. 9.7±0.5 mol/L; $p < 0.001$). On the other hand, tHcy levels in the TT genotype were relatively, but not significantly elevated in comparison with CC and CT genotypes in Japanese (12.7±0.6 mol/L vs. 11.6±0.2 mol/L; $p = 0.09$).

In this study, we showed that serum folate concentration was independently correlated with tHcy ($p = 0.007$) and that the TT genotype of C677T/MTHFR had tHcy levels almost twice as high as the CC and CT genotypes in the Kazakh. In the Republic of Kazakhstan, which is located in central Asia, because the cultural roots of the Kazakh people (60% of the population) are nomadic, the traditional diet mainly consists of meat, such as mutton and beef, and vegetable intake tends to be deficient, particularly in rural areas, due to insufficient distribution. In our current study, 65.4% of the Kazakh participants showed low folate concentrations. This suggests that effective supplementation of folic acid is needed in this area.

Several studies showed that higher dietary folate intake is associated with lower tHcy levels in adults, independent of other dietary factors.^{11,12} However, these studies have mainly been conducted in developed areas such as Western Europe and the USA, and there have been few reports on populations with low folate intake. In this study, we showed that serum folate was significantly correlated with tHcy in the Kazakh, which suggest that appropriate folate supplementation will be effective to control the Hcy status of the population in this area.

Furthermore, our current study shows that tHcy levels in participants with the TT genotype of C677T/MTHFR were almost twice as high as those of participants with the CC and CT genotypes in the Kazakh. On the other hand, tHcy levels in the TT genotype were not signifi-

cantly elevated in subjects with CC and CT genotypes in the Japanese. Recently, Casas *et al.* reviewed the association between C677T/MTHFR genotype and Hcy concentrations, and reported that the weighted mean difference in homocysteine concentration between TT and CC homozygous was 1.93 mol/L in normal subjects.¹³ However, differences ranged widely from -1.30 mol/L to 11.30 mol/L and only two of forty-one studies have shown an over 10.0 mol/L differences between TT and CC homozygous individuals. In the Kazakh, tHcy concentrations adjusted for age, sex in TT and CC homozygous individuals were 19.6±1.8 mol/L and 10.7±0.5 mol/L, respectively, which is a difference of 10.0 mol/L. On the other hand, in the Japanese, tHcy concentrations adjusted for age, sex in TT and CC homozygous individuals were 12.7±0.6 mol/L and 11.5±0.2 mol/L, respectively, which is a difference of only 1.2 mol/L. Other than different assay conditions, contributing factors such as races, daily lifestyle, including the diet should be considered in order to evaluate the association between Hcy and the C677T/MTHFR genotype.

There are several limitations to our study. Since the number of TT genotype of Kazakh and Japanese were only 15 and 17, respectively, further sample collection will be needed. Also we need to evaluate other polymorphisms in MTHFR, such as A1298C.

In conclusion, our results suggest that appropriate supplementation of folic acid would be effective to improve Hcy, as well as folate conditions in Kazakh. Furthermore, C677T/MTHFR is strongly related to tHcy concentration with low folate status. Further studies are needed to outline the procedures for effective supplementation of folic acid in Kazakh individuals.

ACKNOWLEDGEMENTS

This work was supported by a Grant-in-Aid from the Japan Society for the Promotion of Science (No. 16370106, 16406020 and 17590546). We would also like to thank Miss Miho Yoshida for technical assistance with this study.

AUTHOR DISCLOSURES

Ainur Akilzhanova, Noboru Takamura, Yosuke Kusano, Ludmila Karazhanova, Shunichi Yamashita, Hiroshi Saito and Kiyoshi Aoyagi, no conflicts of interest.

REFERENCES

1. James SJ, Pogribna M, Pogribny IP, Melnyk S, Hine RJ, Gibson JB, Yi P, Tafoya DL, Swenson DH, Wilson VL, Gaylor DW. Abnormal folate metabolism and mutation in the methylenetetrahydrofolate reductase gene may be maternal risk factors for Down syndrome. *Am J Clin Nutr.* 1999; 70:495-501.
2. Eichholzer M, Tonz O, Zimmermann R. Folic acid: a public-health challenge. *Lancet.* 2006;367: 1352-61.
3. Lumley J, Watson L, Watson M, Bower C. Periconceptional supplementation with folate and/or multivitamins for preventing neural tube defects. *Cochrane Database Syst Rev.* 2001; CD001056.
4. de Bree A, Verschuren WM, Kromhout D, Kluijtmans LA, Blom HJ. Homocysteine determinants and the evidence to what extent homocysteine determines the risk of coronary heart disease. *Pharmacol Rev.* 2002;54:599-618.
5. Clarke R, Collins R. Can dietary supplements with folic acid or vitamin B6 reduce cardiovascular risk? Design of clinical trials to test the homocysteine hypothesis of vascular disease. *J Cardiovasc Risk.* 1998;5:249-55.
6. Voutilainen S, Rissanen TH, Virtanen J, Lakka TA, Salonen JT; Kuopio Ischemic Heart Disease Risk Factor Study. Low dietary folate intake is associated with an excess incidence of acute coronary events: The Kuopio Ischemic Heart Disease Risk Factor Study. *Circulation.* 2001;103:2674-80.
7. Klerk M, Verhoef P, Clarke R, Blom HJ, Kok FJ, Schouten EG; MTHFR Studies Collaboration Group. MTHFR 677C->T polymorphism and risk of coronary heart disease: a meta-analysis. *JAMA.* 2002;288:2023-31.
8. Rosenberg N, Murata M, Ikeda Y, Opare-Sem O, Zivelin A, Geffen E, Seligsohn U. The frequent 5,10-methylenetetrahydrofolate reductase C677T polymorphism is associated with a common haplotype in whites, Japanese, and Africans. *Am J Hum Genet.* 2002;70:758-62.
9. Akilzhanova A, Takamura N, Zhaojia Y, Aoyagi K, Karazhanova L, Yamashita S. Kazakhstan: a folate-deficient area? *Eur J Clin Nutr.* 2006;60:1141-3.
10. Akilzhanova A, Takamura N, Aoyagi K, Karazhanova L, Yamashita S. Effect of B vitamins and genetics on success of in-vitro fertilisation. *Lancet.* 2006;368:200-1.
11. Rasmussen LB, Ovesen L, Bulow I, Knudsen N, Laurberg P and Perrild H. Folate intake, lifestyle factors, and homocysteine concentrations in younger and older women. *Am J Clin Nutr.* 2000;72:1156-63.
12. de Bree A, Verschuren WM, Blom HJ and Kromhout D. Association between B vitamin intake and plasma homocysteine concentration in the general Dutch population aged 20-65 y. *Am J Clin Nutr.* 2001;73:1027-33.
13. Casas JP, Bautista LE, Smeeth L, Sharma P and Hingorani AD. Homocysteine and stroke: evidence on a causal link from mendelian randomisation. *Lancet.* 2005;365:224-32.

Short Communication

Association between C677T/MTHFR genotype and homocysteine concentration in a Kazakh population

Ainur Akilzhanova MD PhD¹, Noboru Takamura MD PhD², Yosuke Kusano MD PhD³, Ludmila Karazhanova MD PhD¹, Shunichi Yamashita MD PhD², Hiroshi Saito MD PhD² and Kiyoshi Aoyagi MD PhD²

¹Department of Therapy №2, Semipalatinsk State Medical Academy, Semipalatinsk, Republic of Kazakhstan ²Nagasaki University Graduate School of Biomedical Sciences, Nagasaki, Japan and ³Nagasaki Wesleyan University, Nagasaki, Japan

一個哈薩克族群之 C677T/MTHFR 基因型與同半胱胺酸濃度的關係

近來，我們認為由於蔬菜攝取不足，在哈薩克人中可能有低葉酸以及輕微的同半胱胺酸血症的問題存在。為釐清哈薩克族群中同半胱胺酸濃度的決定因素，我們測定 110 位哈薩克人的血清葉酸、白蛋白、肌酸酐、維生素 B12 的濃度及 C677T/MTHFR 基因型，並且與血漿中總同半胱胺酸濃度作比較。在哈薩克，校正了年齡及性別之後，葉酸與血漿總同半胱胺酸有關，TT 基因型者其濃度幾乎是 CC 以及 CT 基因型的兩倍高 (19.7±1.8 mol/L vs. 10.7±0.5 mol/L, $p < 0.001$)。我們的結果顯示，在這個族群中 C677T/MTHFR 基因型與同半胱胺酸濃度之間是有關聯性的，而這個關聯性可能藉由其他因子，例如葉酸狀態，而被影響。

關鍵字：葉酸、同半胱胺酸、哈薩克、5,10-次甲基四氫葉酸還原酶

エ
マ
ー
ジ
ェ
ン
シ
ー
・
ケ
ア

エマージェンシー・ケア

EMERGENCY CARE

2008

Vol.21 No.10 (10月号) (通巻266号)

MC メディカ出版

今日からできる

救急・ICUでの創傷ケア

特集

8

創傷ケアに必要なドレッシング材 と薬剤の知識

吉本 浩

よしもと ひろし

長崎大学医学部形成外科助教

〒852-8501 長崎県長崎市坂本1丁目7-1

秋田定伯

あきた さだのり

同 助教

平野明喜

ひらの あきよし

同 教授

はじめに

従来、創部は消毒とガーゼ保護を行い、乾燥して治癒させるということが一般的な創傷ケアの方法であった。しかし1962年、Winter GD博士のNature¹⁾発表のころから、創部を湿潤環境下で治癒させるモイスト・ウインド・ヒーリング（湿潤療法）という創傷治療理論に変わってきた。それに伴い、さまざまなドレッシング材および薬剤が開発・販売された。これらは有効性を示したものが多く、種類が多いため適切な選択に迷うことがあり、しかも誤った選択をすると創傷治療が遅延するのみならず悪化することもある。適切な創傷ケアを行うには、創傷の状態を正確に評価・判断することに加え、正しいドレッシング材と薬剤の知識が必要である。

ガーゼドレッシングについて

今まで、ガーゼがドレッシング材として広く

用いられてきたのは、ガーゼは安価で入手が容易などの利点に加え、創部を乾燥させて治すという理論にかなっていたからである。

しかし、ガーゼは、創部の湿潤環境保持、保温や外部からの汚染防止など創傷治療を促進するためのすべての基準を満たしていないことが分かっている¹⁾。具体的には、ガーゼで創部を覆うと、滲出液は毛細管現象によりガーゼに吸収および蒸散され、創部が乾燥する。乾燥した創部では、再生しつつある上皮が壊死に陥り、ガーゼが壊死あるいは肉芽組織に固着し、ガーゼ交換時に新たな損傷を創部に与える。また、外部からの汚染や細菌の侵入も防げず、創部の熱もガーゼを通じて逃げていく。

このようなガーゼの欠点を補うためには、塗布する軟膏剤の量を多くしたり、ガーゼをポリウレタンフィルムで被覆することなどの工夫が必要である²⁾。

ドレッシング材について

現在使用されているドレッシング材の多くは、ガーゼの欠点を解消するために、モイスト・ウンド・ヒーリングの創傷治療理論に基づき開発された。つまりドレッシング材の基本的な機能は、創部の適度な湿潤環境と温度の保持や外部からの汚染防止などにより創部の創傷治療を促進することである。また、創部を密閉することによる疼痛緩和効果や過度な滲出液を吸収しコントロールすることにより処置回数の減少などの機能も求められる。しかし、創面を半閉鎖することにより、感染を生じる危険性があり、どの創部に、どの時期に、どのドレッシング材を選択するか、あるいはドレッシング材を使用せず薬剤を選択するかを適切に判断する必要がある。

ドレッシング材の選択

ドレッシング材の選択には、まず創部の正確な観察が必要である。具体的には、創の深さ、滲出液の量、出血の有無、炎症や感染の有無、壊死組織の有無などの状態を観察し、創部を評価する。創感染を認める場合は一般的にドレッシング材の適応となることはない。壊死組織がある場合は外科的デブリードメントが第1選択だが、壊死組織を自己融解する目的でドレッシング材を使用することがある。感染がなく壊死組織もない創部は、創部の深さと滲出液の量によりドレッシング材を選択する。

滲出液や湿潤環境をコントロールする機能でドレッシング材を分類すると4種類に分かれる(表1)²⁾。創部は過度の湿潤環境では周囲の皮膚が浸軟し、皮膚のバリア機能や耐久性が低下

表1 ドレッシング材の分類

- | |
|------------------------------|
| 1. 創面を閉鎖し創面に湿潤環境を形成するドレッシング材 |
| ・ハイドロコロイド |
| 2. 乾燥した創を湿潤させるドレッシング材 |
| ・ハイドロジェル |
| 3. 滲出液を吸収し保持するドレッシング材 |
| ・ハイドロポリマー |
| ・ポリウレタンフォーム |
| ・ハイドロファイバー |
| ・アルギン酸塩 |
| ・キチン |
| 4. その他 |
| ・ポリウレタンフィルム |

するので、的確なドレッシング材の選択が必要である。

主なドレッシング材の特徴

ドレッシング材の分類は材質や形態などによりいくつか分類されるが、ここでは材質によるそれぞれのドレッシング材を表2にまとめた。ポリウレタンフィルム(図1)

ポリウレタンフィルムに粘着剤を塗布したドレッシング材である。水蒸気はフィルムを透過できるが、液体や細菌は透過できない半透過性であり、色は透明あるいは半透明である。シャワー浴も可能で創部の観察も容易である。

浅く感染のない創傷、擦過傷や縫合創あるいはカバードレッシングとして使用される。主に滲出液は少量の場合に使用される。

ハイドロコロイド(図2)

創面に接する部位は、親水性および疎水性ポリマーからなり、外側はポリウレタンフィルムからなる。親水性ポリマーが滲出液を吸収、ゲル化し創面を保護する。

真皮あるいは皮下組織に至る創傷で、滲出液

表2 主なドレッシング材

使用材料	製品名	保険償還	
ポリウレタンフィルム	優肌パーミエイド [®] テガダーム [™] トランスベアレントドレッシング オブサイト [®] ウインド, IV3000ドレッシング バイオクルーシブ [®]	処置料に含む	
ハイドロコロイド	デュオアクティブ [®] ET テガソープ [™] ライトハイドロコロイドドレッシング アブソキュア [®] ーサジカル	真皮に至る創傷 保険償還価格：8円/cm ²	
ハイドロジェル	ビューゲル [®] , ニュージェル [®]		
ポリウレタンフォーム	ハイドロサイト [®] 薄型		
キチン	ベスキチン [®] W		
ハイドロコロイド	コムフィール [®] アルカスドレッシング コムフィール [®] ペースト デュオアクティブ [®] CGF アブソキュア [®] ーウインド テガソープ [™] ハイドロコロイドドレッシング		皮下組織に至る創傷 保険償還価格 標準型：14円/cm ² 異形型：37円/cm ²
ハイドロジェル	グラニューゲル [®] , ジェリパーム [®] イントラサイト [®] ジェルシステム		
ハイドロポリマー	ティエール [®]		
ポリウレタンフォーム	ハイドロサイト [®] , ハイドロサイト [®] AD		
ハイドロファイバー	アクアセル [®] , アクアセル [®] Ag		
アルギン酸塩	アルゴダーム [®] , カルトスタット [®] , ソープサン [®]		
キチン	ベスキチン [®] W-A		
ポリウレタンフォーム	ハイドロサイト [®] キャビティ	筋肉や骨に至る創傷 保険償還価格：25円/cm ²	
キチン	ベスキチン [®] F		

文献2より引用改変

は少量から中等量のときに使用される。

ハイドロジェル (図3)

ポリマーの網目構造内に多量の水分を保持したゲル状あるいはシート状である。乾燥した創の湿潤環境維持や壊死組織を浸軟させるために

使用する。

滲出液が少量の真皮あるいは皮下組織までに至る創傷に使用される。

ハイドロポリマー (図4)

親水性ポリウレタンポリマーと少量のアクリ



図1 ポリウレタンフィルム
 オブサイト®ウンド (スミス・
 アンド・ネフュー ウンド マネ
 ジメント提供)

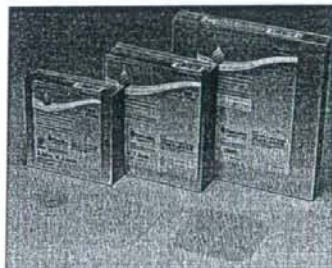


図2 ハイドロコロイド
 デュオアクティブ®ET (プリス
 トル・マイヤーズ スクイブ提供)



図3 ハイドロジェル
 イントラサイト®ジェル(ス
 ミス・アンド・ネフュー
 ウンド マネジメント提供)

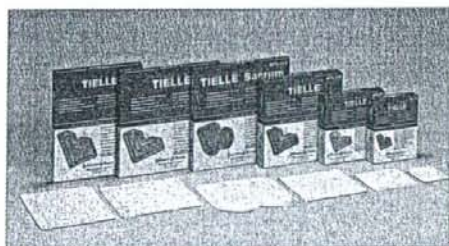


図4 ハイドロポリマー
 ティエール® (ジョンソン・エンド・ジョン
 ソン提供)



図5 ポリウレタンフォーム
 ハイドロサイト® (スミス・ア
 ンド・ネフュー ウンド マネジ
 メント提供)

ルポリマーからなる多孔構造で、中間は不織布
 吸収シート、外側はポリウレタンカバーフォー
 ムからなる。ポリマーは滲出液を吸収するとゲ
 ル化せずに膨張して創面にフィットする。

滲出液が中等量あるいは多量の真皮、ある
 いは皮下組織までに至る創傷に使用される。

ポリウレタンフォーム (図5)

創面に接する部分は非固着性のポリウレタン、
 中間層は親水性ポリウレタンフォーム、外側がポ
 リウレタンフィルムからなる。親水性ポリウレタ
 ンフォームは厚さが5mmのものもあり、高い吸
 収能と創部にかかる圧力を軽減する。

シート状のものは、滲出液が中等量あるいは
 多量の真皮や皮下組織までに至る創傷に使用さ
 れる。

裁断した親水性ポリウレタンフォームを非固
 着性の多孔性立体構造フィルムの袋に詰めたも
 のは筋、骨までに至る創傷に使用される。滲出
 液によって外層が変色するので交換時期が分か
 りやすい。

ハイドロファイバー (図6)

親水性ポリマーであるカルボキシルメチルセ
 ルロースを不織布にしたもので、自重の25倍
 という水分吸収能があり、ゲル化する。

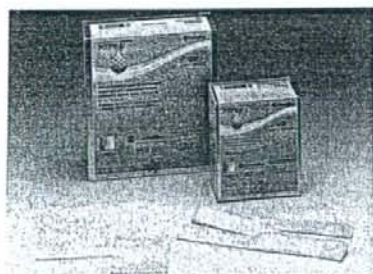


図6 ハイドロファイバー

アクアセル® (プリストル・マイヤーズ スクイブ提供)

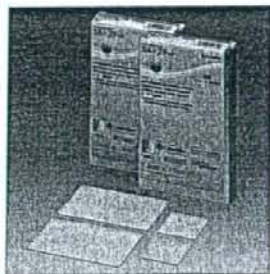


図7 アルギン酸塩

カルトスタット® (プリストル・マイヤーズ スクイブ提供)

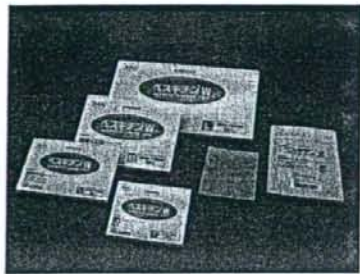


図8 キチン

ベスキチン®W (ユニチカ提供)

滲出液が中等量あるいは多量の皮下組織までに至る創傷に使用される。最近、日本でも抗菌作用を持つ銀イオンを組み込んだものが発売された。

アルギン酸塩 (図7)

海藻から抽出されたアルギン酸塩を不織布にしたものでシート状やリボン状などがある。アルギン酸は自重の15～20倍の吸水量があり、滲出液を吸収してゲル化する。ゲル化するときにカルシウムイオンを放出して優れた止血作用を有するので、新鮮外傷で出血を伴う創面にはよい適応となる。

滲出液が中等量あるいは多量の皮下組織までに至る創傷に使用される。

キチン (図8)

カニの甲羅から抽出したムコ多糖類の一種のキチンを材料として不織布状タイプ、スポンジタイプからなる。滲出液の吸収性と保持能に優れている。

滲出液が中等量あるいは多量の真皮、皮下組織あるいは筋、骨までに至る創傷に使用される。

表3 ドレッシング材の保険償還

- ・ポリウレタンフィルムは処置料に含まれ、保険請求できない
- ・いずれのドレッシング材も2週間を標準として3週間を限度として算定できる
- ・連続して複数のドレッシング材を用いた場合も3週間を限度とする
- ・同一部位に複数のドレッシング材を使用した場合は、主として使用したドレッシング材のみ算定できる
- ・適応として認められている以外の深さに使用したドレッシング材は算定できない

ドレッシング材の保険償還

使用したドレッシング材の保険償還は表3の通りである。

薬剤について

軟膏剤は主薬とそれを保持する基剤から構成され、そのうち基剤は軟膏剤容量のほとんどを占める。そのために、基剤が創の環境に与える影響は大きく、軟膏剤の主薬の選択だけでなく、基剤も考慮した軟膏剤の選択が必要である。

皮膚創部に使用される外用薬によく使用される基剤は主に3種類である(表4)。油脂性基剤